GEOLOGICA CARPATHICA, 2025, 76, 1, 3–22 https://doi.org/10.31577/GeolCarp.2025.01

Numerical modeling of collapsed deep-seated gravitational slope deformations: Insights from the Veľká Fatra Mts., Western Carpathians

ANDRIUS TOLOČKA[1,2], VERONIKA KAPUSTOVÁ[1,✉], ALI MORTAZAVI[2] and MICHAL BŘEŽNÝ[1]

[1]University of Ostrava, Faculty of Science, Department of Physical Geography and Geoecology. Dvořákova 7, Ostrava, Czechia
[2]Nazarbayev University, School of Mining and Geosciences. Kabanbay Batyr Ave. 53, Astana, Kazakhstan

(Manuscript received September 3, 2024; accepted in revised form March 3, 2025; Associate Editor: Rastislav Vojtko)

Abstract: Although deep-seated gravitational slope deformations (DSGSDs) are common, they are not highly investigated phenomena worldwide. In the Carpathian mountain range, they played an important role during the Quaternary evolution of typical core mountain ridges formed by a crystalline basement and surrounded by Mesozoic deposits. There is evidence that the majority of the largest catastrophic rock slope failures (collapses) in the Carpathians appeared precisely in areas affected by DSGSDs. Two DSGSD-affected slopes in the northeast part of the Veľká Fatra Mts. (Western Carpathians, Slovakia) have recently been subjected to a detailed investigation involving geomorphic mapping, remote sensing analysis, structural data collection, and numerical modeling. To improve our understanding of these gravity-induced processes, we performed a back-analysis of collapsed DSGSDs through a continuum-based, finite-element model composed using the RS2 code. Results show that these DSGSDs are strongly predisposed by regional geological structures given by the intersection of bedding planes, joint sets, and thrust faults. The numerical modeling approach and performed back-analysis have enabled a better view of the development of these deep-seated slope failures in the Veľká Fatra Mts. It suggests a high diversity of mechanisms leading to the origin of these DSGSD cases. The main causal factors influencing their development have been bedrock structure, the lithological composition (dolomite and limestone), thrust faults, and deep weathering of the rock mass. Both cases have deep basal shear zones, as well as a small number of series of gravitational faults associated with complex joint sets.

Keywords: Carpathian Mountain range, Veľká Fatra Mts., DSGSD, numerical modeling, back-analysis

Introduction

Deep-seated gravitational slope deformations (DSGSDs) are large-scale mass movements that can have a wide range of geomorphic and geologic characteristics. They can occur in a wide range of topographic settings, as well as in many rock types (Dramis & Sorriso-Valvo 1994; Crosta 1996; Pánek et al. 2011). The primary characteristics of these processes are the lack of a continuous sliding surface and the existence of a deep basal deformation zone where displacement mostly occurs as a result of rock microfracturing (Radbruch-Hall 1978; Lebourg et al. 2014). They are referred to by various names, including sackung, gravity faulting, deep-reaching gravitational deformation, deep-seated creep deformation, gravitational block-type movement, gravitational spreading, and gravitational creep (Malgot 1977; Discenza & Esposito 2021). DSGSDs have been documented practically everywhere in the world: from lowlands and mountains to the sea floor and even on Mars's surface (Kromuszczyńska et al. 2019). In general, they are characterized by typical superficial morphological features distributed along the entire mountain system, mostly including the ridges, slopes, and valleys (Discenza et al. 2021). In most DSGSDs, it is quite difficult to recognize continuous sliding surfaces or basal shear zones, which are the typical elements of landslides. According to the type of indicative movement processes, DSGSDs are divided into sackung style deformation, lateral spreading of ridges, and spreading of thrust fronts (Sorriso-Valvo et al. 1999). Gravitationally deformed slopes often host rockslides or smaller-scale, deep-seated landslides, which pose a serious landslide hazard. As a result of the prolonged timespan involved and the frequent obliteration of the surface gravitational features produced by DSGSD by weathering and erosion, the process of slope deformation leading to a collapse (fast mass movement) is not well understood (Agliardi et al. 2013).

This research focuses on two DSGSD cases (Brdo Mt. and Žľabiny Mt.) in the NE part of the Veľká Fatra Mts., Western Carpathians, located in Slovakia (Fig. 1). In the region, a small number of large-scale deformations were detected by interpreting the LIDAR digital terrain model (DTM) and by observing the surface features (grabens, scarps, antislope scarps, troughs, and landslides) in the field. The bedrock consists mainly of Triassic–Cretaceous faulted and folded limestones and dolomites. It forms the ideal conditions for the development of diverse gravitational deformations and landslide types (Briestenský et al. 2011).

✉ corresponding author: Veronika Kapustová
veronika.kapustova@osu.cz

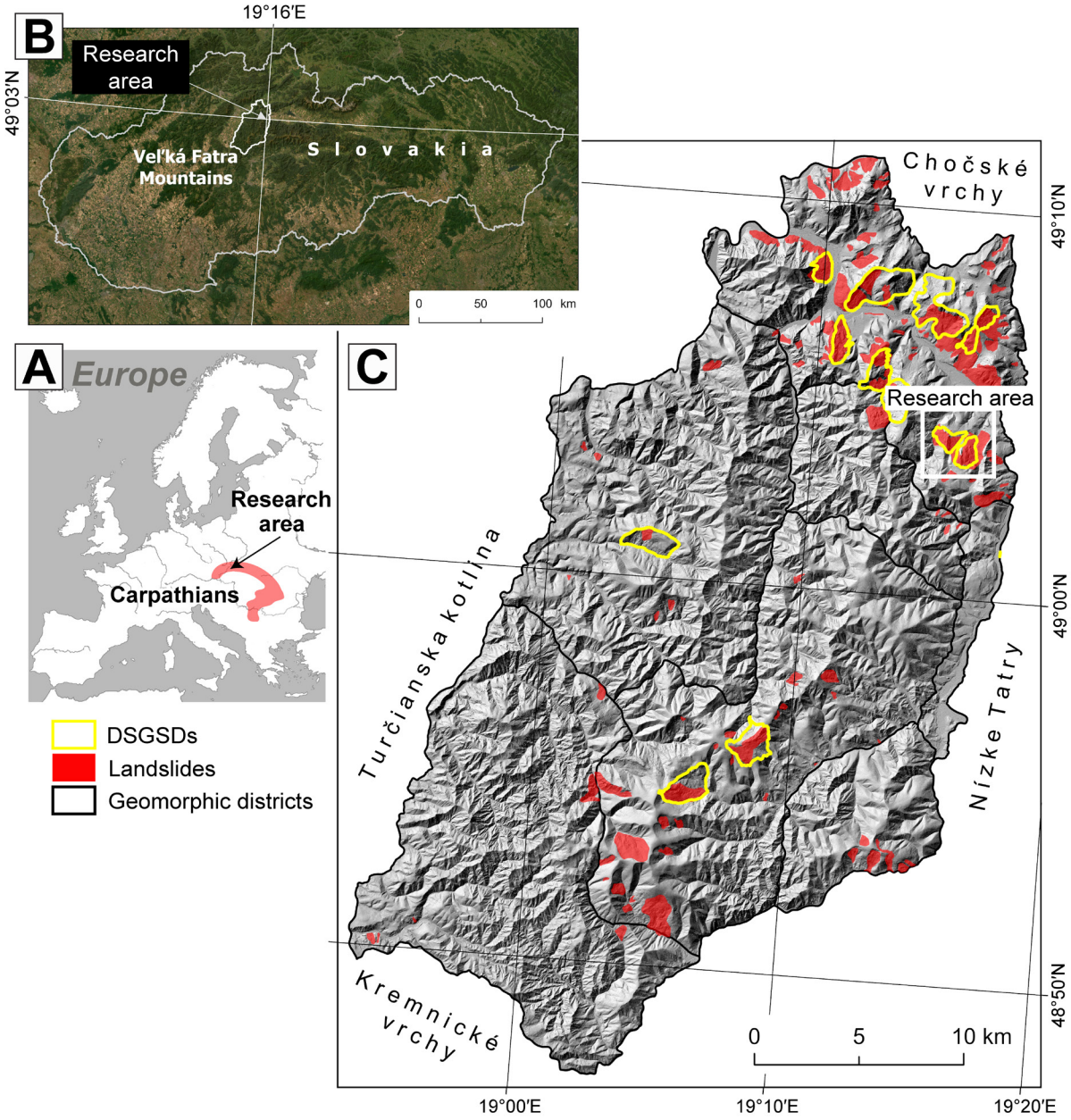

Fig. 1. A — Location of the study area in Europe and Carpathians. **B** — The satellite image shows the location of the study area and Veľká Fatra Mts. in Slovakia (GKÚ Bratislava, NLC 2024). **C** — Hillshade map of Veľká Fatra Mts. shows the main landslide (according to Šimeková & Martinčeková 2006) and DSGSD areas (according to authors).

In this work, we aim to introduce a multi-technique methodology combined with field observations, structural, geomorphic, LIDAR data analysis, and numerical modeling, which could be helpful for a more holistic understanding of the transition from DSGSD to its collapse. Numerical modeling was performed to investigate the development and characteristics of collapsed DSGSDs, as well as to reconstruct the initial conditions and ensuing stages of the deformation. We present an analysis of a mountain massif affected by a large-scale DSGSD, which will allow us to evaluate stress and strain fields, displacement rates, and magnitudes in the different stages of deformation development. This case study shows well-preserved gravitational morphostructures in a relatively isolated rock massif. However, the high local relief (>400 m) geometry and volume of the massif prevent us from using traditional limit equilibrium slope stability models. In this study, we perform a complete stress analysis using the finite element method, which reveals the main predisposing factor for DSGSD collapse in retrospective analysis and allows for the prediction of the most probable areas and slip zones/surfaces for future slope collapses in the research site.

The objectives of this paper are as follows: (i) to characterize DSGSDs from a geological, geomorphological, and geomechanical point of view; (ii) reconstruct the original slope

and, after geomechanical characterization of the geological materials and hydrogeological conditions, analyze the slope failure using a 2D numerical model to identify the factors and causes that have controlled the development of the landslide (back analysis); (iii) integrate the process of DSGSD evolution within the context of the geomorphological evolution of the Veľká Fatra Mts.

Regional background

Malinô Brdo study area

The Malinô Brdo area is located in the northeastern Veľká Fatra Mts. (a part of the Western Carpathians) foothills and contains a small number of partially-isolated, low mountain massifs which are dissected by small river valleys (Fig. 1). The land cover of the study area is mostly forested with some grassland areas on the ski slopes and valley bottoms, as well as small areas of buildings (mostly ski resorts and summer houses; Fig. 2). The area is located in the greater surroundings of the town of Ružomberok on the left side of the Váh River southwest of the town. Approximate geographical coordinates are 49°04'N and 19°16'E. The altitude of the studied mountain massifs ranges from approximately 600 to 1000 m a.s.l. The study area has a varied bedrock lithology, including carbonate rocks (limestones and dolomites), as well as quartzites and claystones. Among the soil types, brown cambisoils are the most common. For Slovak standards, the study area is cool (the average temperature during the warm season is 10–15 °C, while during the cold season it ranges between −5 and 5 °C) and wet (Lepeška 2016). The local drainage network is characterized by the SW to NE-oriented Zajakovo, Hrabovský potok, and Čutkovský potok brooks, which flow northwards into the NW to SE-oriented Váh River.

Geology of the study area

The Veľká Fatra Mts., with an area of 784 km^2, belong to the Central Western Carpathians and are situated in north-central Slovakia (Kočický & Ivanič 2011). The mountain belt was formed during the Alpine orogeny from the Mesozoic to the Cenozoic era (Kováč et al. 1994; Králiková et al. 2014b). The Veľká Fatra Mts. are typical core mountains with a Tatric crystalline basement and Mesozoic cover that is overlain by two superficial nappes (Földvary 2009; Plašienka 2018). The Tatric crystalline basement is composed predominantly of the Ľubochňa granitoid massif (tonalite, granodiorite, granite, and leucogranite), and it outcrops only to a limited extent. The Variscan age of the granite was determined as 342±4 Ma (Kohút et al. 1996) or 337±3, 332±3 Ma (Kohút & Larionov 2021) respectively. The northern part of the Veľká Fatra Mts. is built by Hronic and Fatric nappes. The tectonically-higher (Triassic) Hronic Unit consists of dolomites and limestones, while the tectonically-lower (Middle Triassic to Lower Cretaceous) Fatric Unit contains both karstified carbonates and argillaceous aquitards. The mountains exhibit complex fold structures due to the intense tectonic forces involved in their formation. Anticlines and synclines are common features in the region. These fold structures give rise to the distinct topography of the mountains, with prominent ridges and valleys (Földvary 2009; Plašienka 2018). Tectonic faults were most likely reactivated during the large-scale neotectonic uplift in the Veľká Fatra Mts. (Maglay et al. 1999; Králiková et al. 2014b).

In general, the thrust sheet karst aquifer of the Hronic Unit is mainly elevated above the erosional base, distinguished from below by thrust fault and argillaceous aquitards of the Fatric Unit. It is dissected by both tectonics and erosion, as well as affected by dissolution (Malík et al. 2019). The dip of the underlying aquitard influences the direction of karst groundwater flow (Bednarik et al. 2010; Malík et al. 2019). This is also true for the hydrogeological structure of our cases: Brdo Mt. and Žľabiny Mt. in the Malinô Brdo study area. The slopes in the study area are predominantly built of Mesozoic rocks (dolomites, limestones, marlstones, clayey limestones, and shales) covered by Quaternary slope deposits (Fig. 3). The karstified Triassic carbonates are overthrusted on an aquitard of Lower Cretaceous clayey limestones.

Mass movements in the Veľká Fatra Mts.

Slope movements are one of the most important geodynamic processes in Slovakia (Western Carpathians). A systematic inventory of landslides in Slovakia started after the Handlová town landslide disaster in 1960–1961 (Matula & Nemčok 1966). In the most recent Slope stability atlas project of Slovakia (Šimeková & Martinčeková 2006), more than 21,190 slope failures (mainly landslides) have been recorded in the Slovak part of the Western Carpathians. They occupy a total area of 2576 km^2, accounting for 5.25 % of Slovakia's total land area (Kopecký et al. 2012). Only 9 % of the affected area shares the core mountain region. However, the majority of the mapped DSGSDs (86 % cases) were found in the core mountains (Šimeková et al. 2014). More than 140 different forms of mass movements were recorded and validated in the northern part of the Veľká Fatra Mts. near the Váh River valley (Fig. 1C). Most landslides here occur in the Mesozoic limestone and dolomite bedrock, which is covered by a thin Quaternary sediment layer.

Materials and methods

Selection of study sites, remote sensing data interpretation, and fieldwork

The Malinô Brdo area (Brdo and Žľabiny DSGSDs, Fig. 2) was chosen for the research of this case study to represent both typically and clearly expressed DSGSDs in the Veľká Fatra Mts. Here, the natural geographical conditions were more

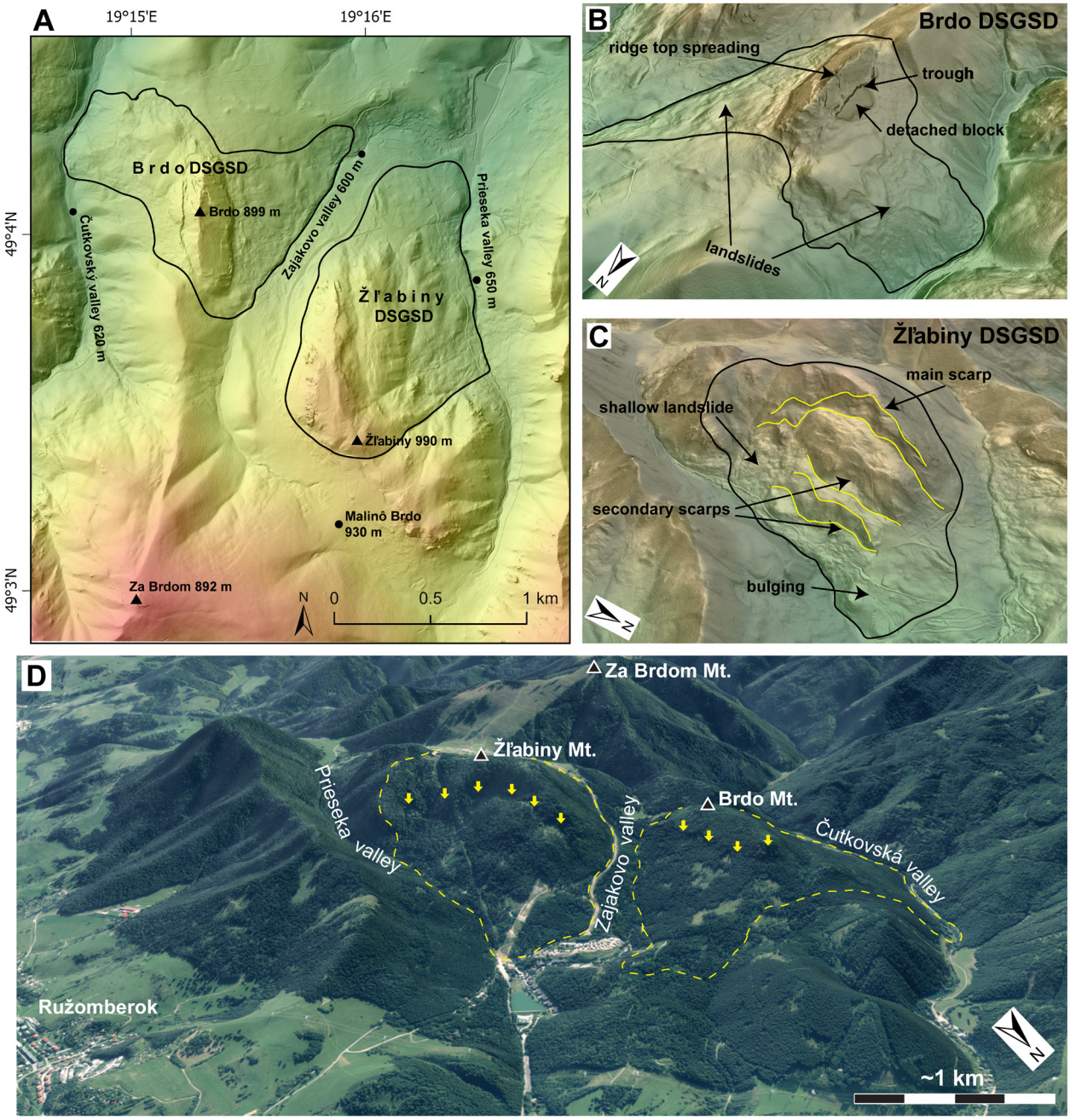

Fig. 2. Geomorphology of the study area. **A** — Hillshade map of Malinô Brdo area with DSGSDs. **B** — 3D hillshade view of Brdo DSGSD. **C** — 3D hillshade view of Žľabiny DSGSD. **D** — 3D orthophoto view of Malinô Brdo area. Yellow dashed lines – DSGSDs areas, yellow arrows – main scarps.

suitable for rock sampling and structural mapping. The territory is suitable for comparing the propagation of DSGSDs with different geometries under the same geological conditions. The surface area was also an important aspect of the decision, because RS2 numerical model accuracy and precision relate to slope complexity and scale, as well as the geological complexity of rock mass. In the Malinô Brdo area, the structural controls made this case more interesting to investigate due to the possibility of evaluating the influence of a thrust fault on DSGSD development.

Initially, the study was carried out through the analysis and interpretation of remote sensing data, such as topographic maps, orthophotos, and DTM provided by the Geodesy, Cartography and Cadastre Authority of the Slovak Republic (GKÚ Bratislava, NLC 2024; ÚGKK SR 2024). The remote study led to the first detection of the landforms used in further analyses (scarps, ridges, gullies, troughs), as well as to preliminary measurements of the main scarp, moved blocks, and landslide debris areas. Primary DTM created from LIDAR point cloud data (filtered from vegetation) was used to create

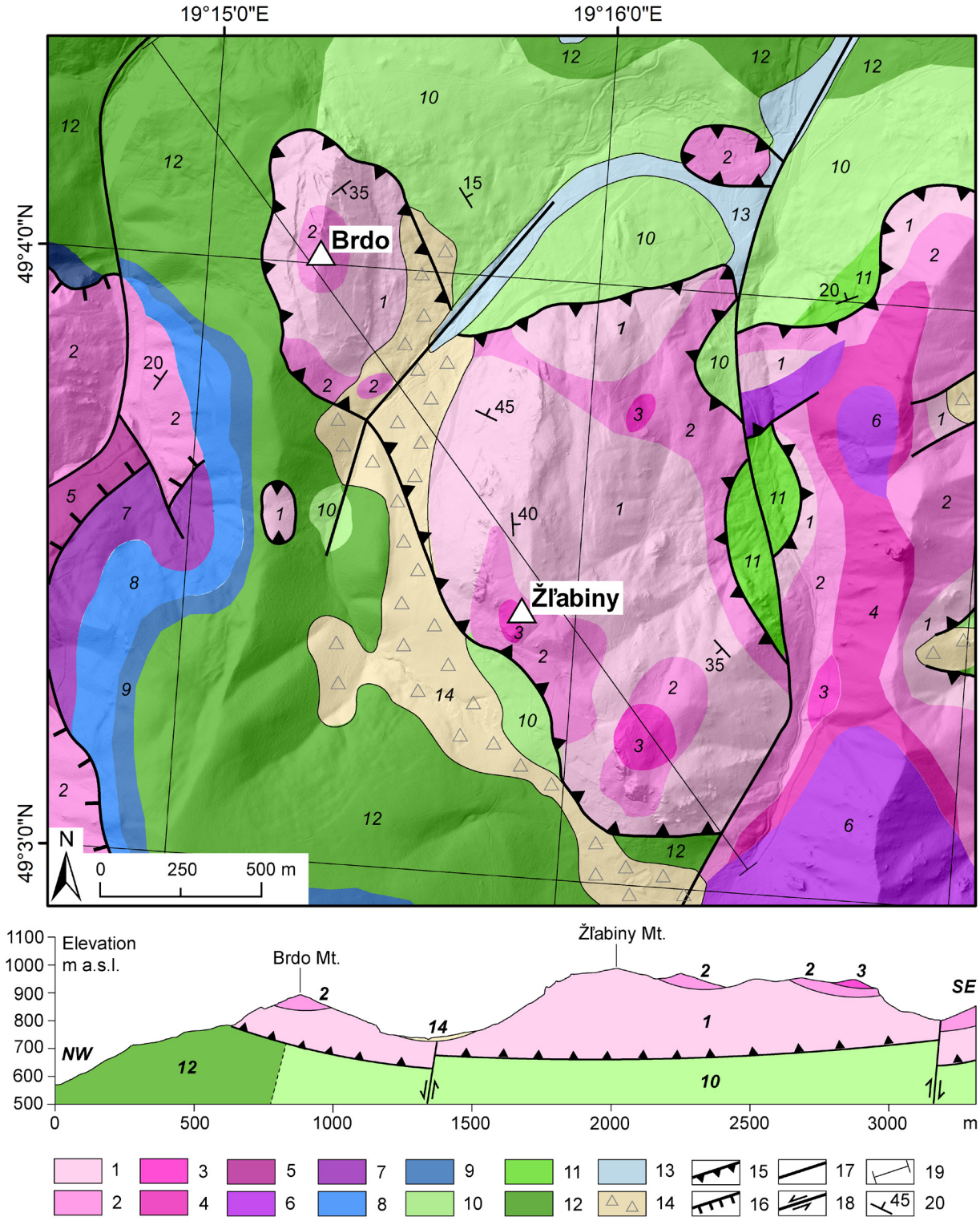

Fig. 3. Simplified geological map and profile of the study area (after Polák et al. 1997). Numbers in the geological profiles correspond to rock types in the legend. Legend: *Hronic Unit (Triassic)*: 1 – Gutenstein limestone; 2 – Ramsau dolomite; 3 – Schreyeralm limestone; 4 – Reifling limestone; 5 – Carpathian Keuper: shales and dolomites; 6 – Hauptdolomit: organodetritic dolomites; 7 – Kössen Fm.: organodetritic limestones, marly limestones and shales. *Fatric Unit (Jurassic)*: 8 – Allgäu Fm.: limestones and shales; 9 – Ždiar Formation: radiolarian limestones and radiolarites. *Fatric Unit (Cretaceous)*: 10 – marly shales and limestones; 11 – Vlkolínec breccias: limestone and marly breccias; 12 – Mraznica Fm.: limestones, marlstones and shales. *Quaternary*: 13 – fluvial sediments; 14 – slope sediments. *Other signs*: 15 – thrust faults; 16 – tectonic reduction lines; 17 – normal faults and other tectonic lineaments; 18 – normal faults (in section only); 19 – a cross-section of the geological profile; 20 – strike and dip of bedding.

a hillshade, slope, topographic curvature, and aspect maps of the DSGSD areas for a better understanding of surface topography and landforms. In both locations, large-scale and small-scale features, such as scarps, antislope scarps, and cliffs, were visible on the derivated maps and were also helpful for detection of these features in the field with dense vegetation cover. The topographic profiles derived from DTM were used in the numerical model as an original surface. The topographic profiles of neighboring mountain ranges helped reconstruct the possible initial surface geometry of Brdo Mt. and Žľabiny Mt. We were able to roughly define the DSGSD collapse limits according to the distribution of landslide deposits on the maps. The mapping of other DSGSDs and landslides in the Veľká Fatra Mts. was also done using remote sensing data.

Field mapping was carried out in 2022 by paying special attention to geological and geomorphological structures bearing essential significance for subsurface gravitational deformation. Structural measurements of discontinuities (dip and dip directions) were obtained throughout the head scarp and upper areas of DSGSDs. The orientation of foliation, bedding planes, and joint surfaces observed at bedrock outcrops was measured. Morphological features associated with DSGSD activity (scarps, extensional fractures, troughs, and tilted blocks) were mapped in the field and digitized with the help of a shaded relief model derived from DTM with a resolution of 1 m. Rock samples were collected for the further characterization of geomechanical properties. Rock strength was measured with a mechanical Schmidt hammer in horizontal and vertical positions on *in situ* rock masses and moved block surfaces, as well as on weathered and intact rock surfaces. The field mapping helped to recognize the boundaries between individual shallow landslides and structural features inside DSGSDs.

Numerical modeling of the study sites

Model assumptions and determination of rock mass design parameters

The finite element code RS2 (Rocscience Inc. 2019) was used to conduct a complete stress-strain analysis. The essential steps of the morphostructural evolution of the Brdo and Žľabiny DSGSDs were reproduced using a sequential analysis of the areas of interest. A sensitivity analysis of the assigned key parameters was performed to calibrate the in-situ properties of the rock mass involved in the deformational process and back-analyses. DSGSD numerical analysis was carried out by integrating information from geotechnical, field, and laboratory investigations, as well as existing data about mass movements and rock mass properties in the Veľká Fatra Mts. During field and laboratory research, the geomechanical properties required for numerical modeling were determined (Table 1).

The rock mass strength envelopes were modeled using the generalized Hoek-Brown criterion (Hoek et al. 2002), which is based on the representative Uniaxial Compressive Strength (UCS) and material constant for the intact rock (mi) values, estimated by Schmidt hammer rebound number correlation with USC, and back-calculated Geological Strength Index (GSI) values. They characterize the quality of the rock mass in terms of the degree of fracturing and the physical condition of discontinuities (Hoek et al. 2013; Bertuzzi et al. 2016; Wallace et al. 2022). The extended Hoek and Diederichs approach (Hoek & Diederichs 2006) was used to calculate rock mass elastic modulus values based on presumed intact Young's modulus and GSI values. A disturbance factor (D) was assigned to the rock mass due to stress relaxation, where 0 represents in-situ stressed rock mass and 1 represents a significantly disturbed rock mass. The joint parameters were estimated using data from fieldwork and geological maps. The Hoek-Brown criterion was used to determine rock mass design parameters and later to perform a parametric analysis. The estimation of strength and deformability of rock masses was made using the Hoek et al. (2002) and Hoek & Diederichs (2006) approaches, which were parametrized using field estimates of the Geological Strength Index (GSI). The reference UCS of intact rocks was empirically derived from Schmidt hammer measurements on the dolomite and limestone rocks, according to the empirical relation proposed by Wang et al. (2017).

Table 1: The determined rock mass data used in the numerical modelling.

Failure Criterion: Generalized Hoek Brown				Rock mass			
	Parameter	Symbol	Unit	Ramsau dolomites	Gutenstein limestones	Marly shales	Marly limestones
Intact rock	Uniaxial Compressive Strength	UCS	MPa	50	60	35	40
	Geological Strength Index	GSI	–	35	50	40	40
	Material constant for the intact rock	mi	–	9	12	6	9
	Disturbance factor (D)	D	–	0.5	0.3	0.4	0.35
Insitu rock mass	Reduced material constant	mb	–	0.52	1.47	0.41	0.67
	Tensile Strength		MPa	0.03	0.09	0.04	0.03
	Uniaxial Compressive Strength	UCS	MPa	0.8	2.7	0.7	0.9
	Global Strength		MPa	4.6	9.7	2.9	4.2
	Deformation Modulus	E	GPa	1.5	4.0	1.8	1.9
	Cohesion	c	MPa	1.6	2.8	1.0	1.4
	Friction Angle	φ	°	21.2	29.4	19.6	23.1

Model building

To analyze the slope evolution and the kinematics of DSGSD, a comprehensive numerical analysis was conducted using the finite element software RS2 (Rocscience Inc. 2019). The geology of the area determined from field analyses was implemented into the RS2 model with reasonable accuracy and the model was constructed in such a way that various stages of deformation could be simulated. This enabled a realistic simulation of deformation mechanisms occurring within the high-relief regions of interest. The model extends from the bottom of the slope (approximately 600 m a.s.l.) in the river valleys up to the top of the mountains (at a height of approximately 900 m a.s.l.). A critical step was the reconstruction of the initial slope geometry before DSGSD collapse. This was done in ArcGIS Pro (Esri 2023) using the topography extrapolation method of DTM in the shape of the nearest Za Brdom Mt., taking into consideration the main tectonic features of the area. Afterwards, the model geometry was set up assuming the initial slope height of 950 m, which can be considered the representative topography for the Veľká Fatra valleys without the effect of erosion and slope deformations. The sequential numerical analysis was based on a restored geomechanical cross-section, which was then transferred to a numerical domain consisting of a primitive uniform mesh grid with a resolution of approximately 5 m. The numerical domain was laterally extended by approximately 200 m on both the left and right sides of the model, as well as 100 m below the topography to avoid any boundary effects and represent accurate mesh deformation in the valley bottom where toe bulging occurs. Gravitational stress was considered an initial condition. The considered topographic profile is between 500 and 950 m a.s.l. in both the Brdo and Žľabiny cases. Since an infinite half-space was assumed, the horizontal displacements were avoided along the lateral boundaries of the numerical domain, while vertical and horizontal displacements were avoided at the model bottom, and the natural slope surface was free. The master joints were added to represent the main thrust faults, gravitational faults, and previous slip surfaces. The minor joint set was added to some layers of rocks as a representation of existing bedding planes and synclinal structures. History query points were added to the model in critical areas and near the slipping zones to investigate the deformation mechanisms more in detail. Parametric analysis of material and joint properties, such as Young's modulus and friction angle, was performed for both DSGSD cases to evaluate the influence and variation of geomechanical parameters for the model behavior.

In the constructed models of both DSGSDs, four analysis sequences were considered: 1st stage – initial surface geometry without any discontinuity; 2nd stage – initial geometry with fault discontinuities; 3rd stage – initial geometry with main fault discontinuities, minor joint discontinuities, and material boundaries, which separate eroded/displaced material and the current topography; 4th stage – current topography with discontinuities and without eroded/displaced rock mass.

Geology, landforms, and numerical modeling results of DSGSDs

During this research using high-resolution LIDAR data, 10 large-scale DSGSDs were identified in the northern part of the Veľká Fatra Mts. (Fig. 1C). Many of them are found in dolomitic limestone rocks of the Hronic and Fatric tectonic units. Northeast of Ostredok Mt. (1596 m a.s.l.), the highest peak in the Veľká Fatra Mts., a further 2 large-scale DSGSDs were recognized. In total, we mapped 13 possible DSGSD areas in the Veľká Fatra Mts. with areas varying from approximately 0.5 km^2 to more than 4 km^2, where some smaller mass movements are nested (Fig. 1C).

Brdo DSGSD: Stratigraphy, morphostructure, and landslide characteristics

The Brdo Mt. massif is composed of two tectonic units: Triassic formations of the Hronic Unit at the top and Cretaceous formations of the Fatric Unit towards the bottom (Fig. 3). These two units are separated by a thrust fault. The Hronic Unit consists of bedded Ramsau dolomite of Late Anisian age and Gutenstein limestone of Early Anisian age. The Fatric Unit is typically represented by the Mraznica Formation, consisting of clayey limestones, marlstones, and calcareous shales of Valanginian–Early Barremian ages, as well as calcareous shales and limestones of the Late Barremian–Early Albian. Surficial parts of Brdo Mt. are covered by Quaternary deposits, mainly unconsolidated material originating from weathering and landslides, partially covering the sedimentary formations of the Fatric Unit on the eastern slopes of the mountain (Fig. 4). Angular rock debris deposited on slopes has also been observed. Along the slopes, there are numerous Quaternary landslides of several typologies (rock toppling, rock slides, and rock falls).

Brdo Mt. is a morphologically-isolated mountain, symmetric in the N–S direction. Structural measurements taken at various locations of the Brdo DSGSD (Fig. 4A, C) indicate that bedding planes are oriented between S_0 080/23° and S_0 090/25°, with the main fault plane at the surface oriented at 200/85° and 043/30° (all data as dip direction and dip). These planes are found within the Gutenstein limestone in the northern part of the mount, just below the ridge (site b on Figs. 4A, 5B). In the Ramsau dolomite, bedding planes are oriented S_0 060/35° to S_0 070/40° in the central trough on the top of the mount, and the main joints are oriented at 170/70° and 230/80° (site e on Figs. 4A, 5C). The Brdo DSGSD is a typical sackung with double ridges at the top that are several meters deep, as well as hundred-meter-long N–S-oriented trough systems symmetrically on the E and W slopes of the mount, and a NW–SE-oriented trough system crossing the ridge (Figs. 4A, 5C, E, F). Gravity-induced caves were observed in the central trough (Fig. 5D). Numerous fractures and steep slope walls have also formed in the Gutenstein limestone. The affected zone is visible on the slope map of the area (Fig. 4B) with 75–90° steepness along the NW and E slopes of

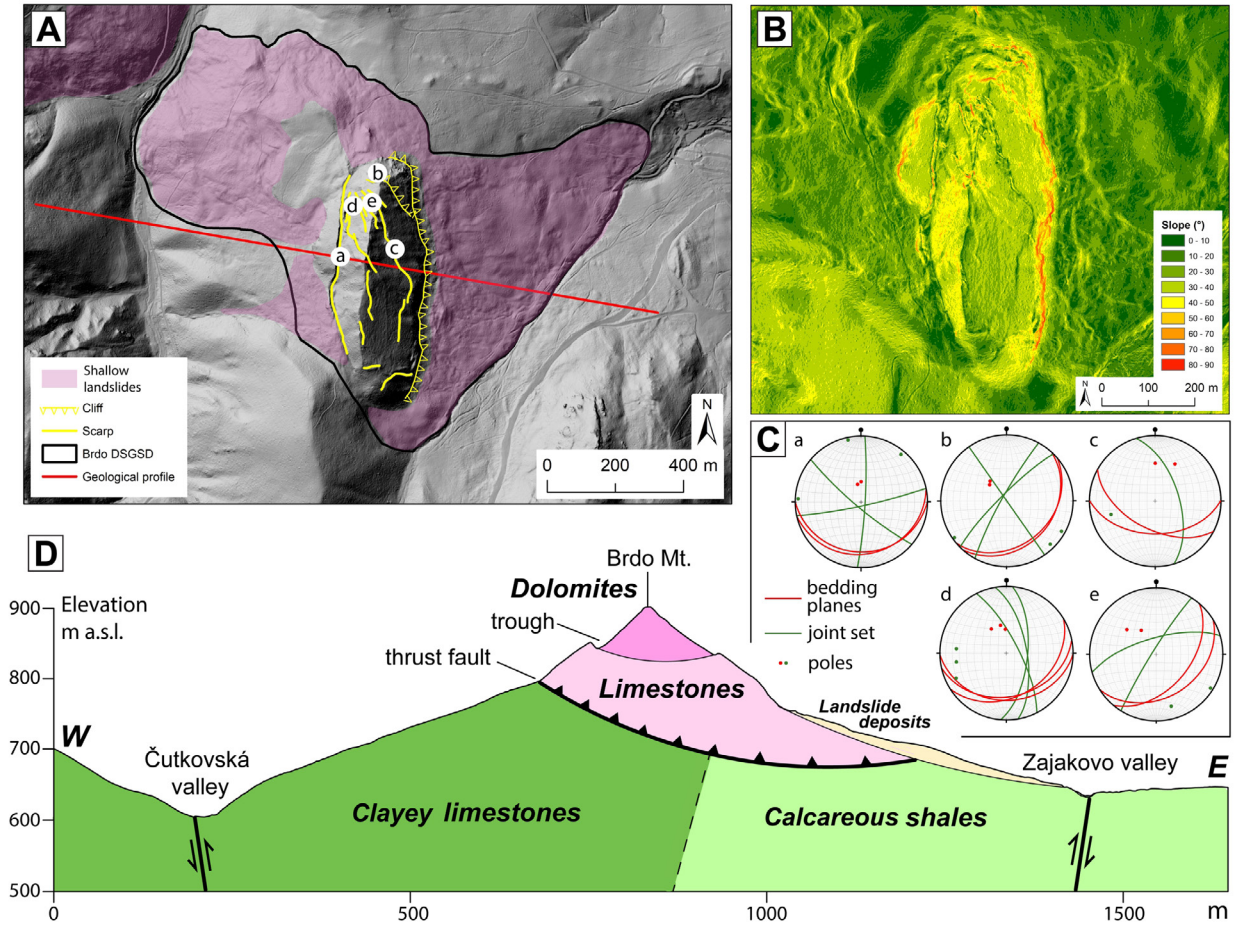

Fig. 4. Brdo DSGSD: **A** — Hillshade map with the main gravitational features. **B** — Slope map. **C** — Plots of main discontinuity systems corresponding to the locations a–e in the hillshade map: a – western trough, b – main scarp below the ridge, c – eastern trough, d, e – central trough. **D** — Simplified geological cross-section. Dashed line shows the assumed rock mass contact surface. Black lines indicate faults.

Brdo Mt. In these zones, most of the rock falls and toppling events occur. The rocks of the Fatric Unit below the contact zone are covered by Quaternary deposits; therefore, structural investigation was not possible.

The Brdo DSGSD varied from 600 to 902 m a.s.l., including the small mountain massif (Fig. 2). The Čutkovský Potok valley limits DSGSD on the west and the Zajakovo valley on the east. From the north, it is limited by Čutkovo Mt. (737 m a.s.l.), and from the south, by Za Brdom Mt. (890 m a.s.l.). Brdo sackung is a complex mass movement around 1×1.3 km, with an asymmetric landslide deposit on the NW and E slopes of the mountain, mainly affecting formations of the Fatric Unit (Fig. 4). In the upper part, the huge limestone and dolomite blocks are detached from the main massif and moved to the sides, forming the main antislope scarps and troughs (Fig. 5). Several smaller blocks of variable size were also observed in the troughs and on the slopes (Fig. 5C). The shape of the blocks is controlled by the sets of discontinuities that affect the rock mass. The rock walls surrounding the slopes of Brdo Mt. (Fig. 4B) could be considered head scarps, because just below them, typical landslide deposits extend with elongated toes to the valley sides. The S and SE slopes of the Brdo DSGSD are least affected by gravitational processes and thus keep the original curvature of the mountain ridge.

Žľabiny DSGSD: Stratigraphy, morphostructure and landslide characteristics

Žľabiny Mt. consists of the Cretaceous Mraznica Fm. (clayey limestones, marlstones, calcareous shales) of the Fatric Unit, which are in a footwall position with respect to the Triassic Gutenstein limestone and Ramsau dolomite of the Hronic Unit of Gutenstein limestones and Ramsau dolomites in a hangingwall position (Figs. 3, 6). From the field observations and orthophotos, it is clear that in the main landslide on the eastern slope, there is a thick layer of slope deposits, which are not shown in the general geological map (Fig. 3). The landslide debris now covers an area of about 1 km^2, mainly formed on the Fatric Unit on the eastern slope and has a typical, hummocky topography with a marked landslide toe. The upper parts of the Hronic Unit display frequent karst features.

The main structural measurements on this site were performed in the upper western part of DSGSD in the troughs and

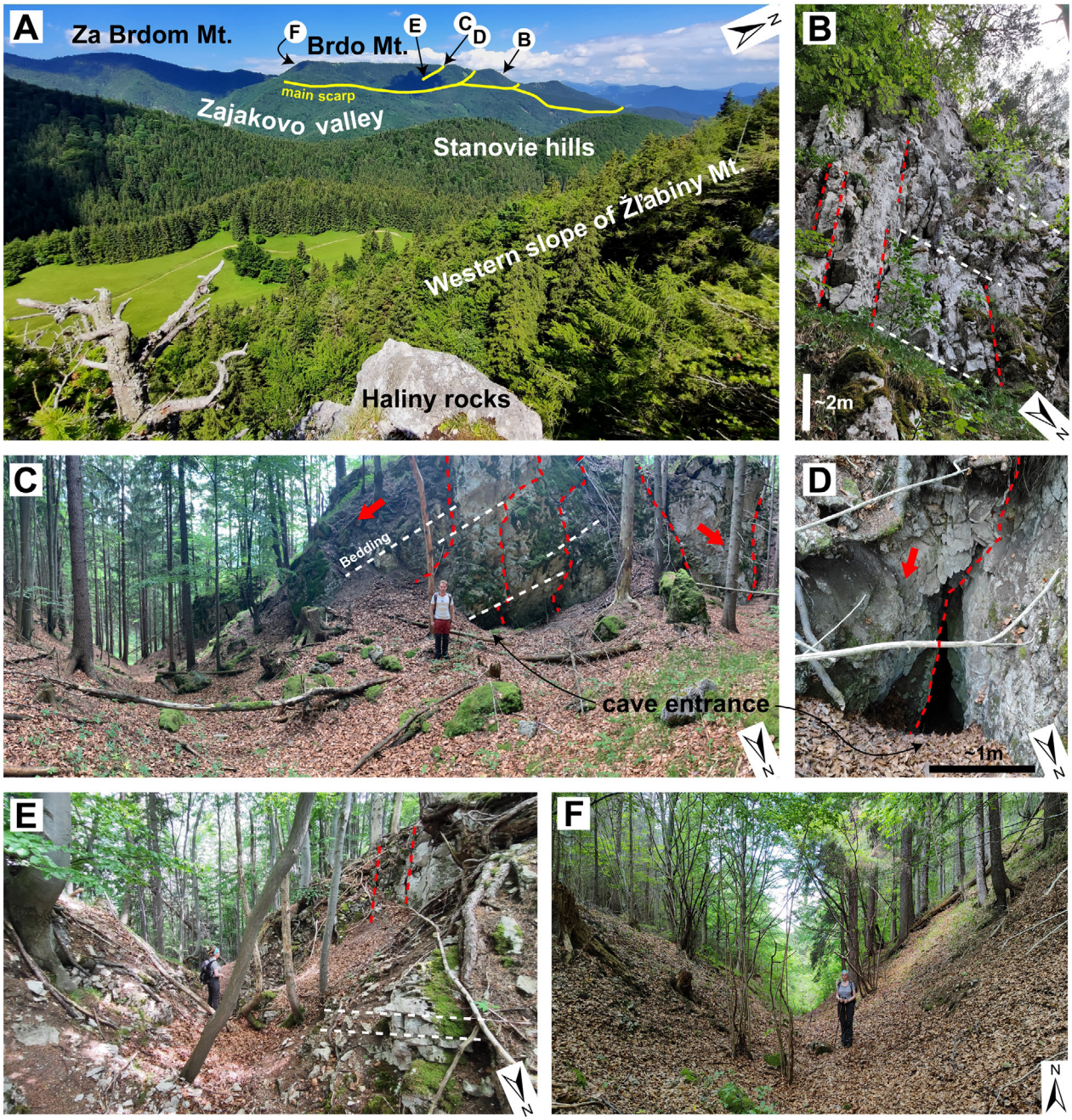

Fig. 5. A — Panoramic view of the Brdo mountain and the surrounding areas. Yellow lines show the main scarp area which separates the upper and lower sectors of DSGSD. Locations of the photos B–F are indicated. **B** — Main scarp wall corresponding to location b in Fig. 4A. White dashed lines – beddings, red dashed lines – main joints. **C** — Central trough in the upper part of DSGSD with separated dolomitic blocks and gravity-induced caves. View corresponding to the location e in Fig. 4A. Red arrows show the assumed movement directions of blocks. **D** — Cave entrance detail. **E** — Main eastern trough corresponding to the location c in Fig. 4A. **F** — Main western trough corresponding to the location a in Fig. 4A.

outcrops on the top of the mountain (Fig. 6A, C). The layers of the Fatric Unit are covered by Quaternary sediments and have no outcrops; therefore, it was impossible to perform any measurement. The formations of the Hronic Unit above the thrust plane show a syncline geometry with layers dipping 40–45° to NE on the western side of the mountain and 35° to SW on the lower eastern side of slopes (Fig. 6A). On the western slopes of Žľabiny Mt., there are numerous blocks tilted and/or moved downslope towards the Zajakovo valley. The joint measurements of *in situ* rock mass (site a on Figs. 6A, C, 7D) show the main two sets of discontinuities: NE–SW-oriented, dipping at about 15° and N–S-oriented, dipping at 80°. The tilted block (site b on Figs. 6A, C, 7D) shows NE–SW-oriented discontinuities with a dip of about 10° and N–S-oriented, with

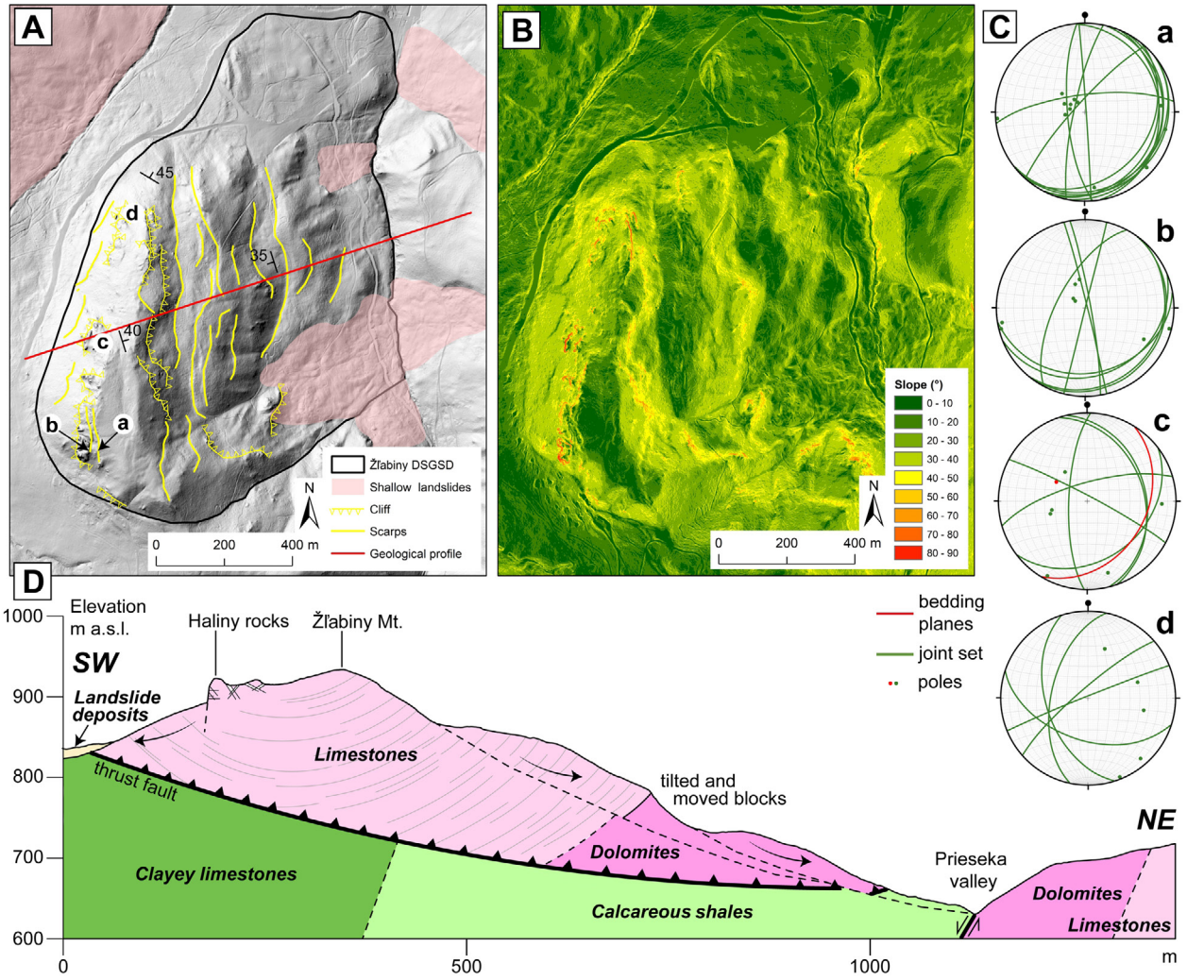

Fig. 6. Žľabiny DSGSD: **A** — Hillshade map with the main gravitational features. **B** — Slope map. **C** — Plots of main discontinuity systems corresponding to the locations a-d in the hillshade map: a – in situ block of Haliny rocks, b – tilted block of Haliny rocks, c – the northern part of Haliny rocks, d – ridge top scarp outcrop. **D** — Simplified geological cross-section. Dashed lines show assumed rock mass contact surfaces. Black lines show faults.

a sub-vertical 85–90° dip angle. At the top of Žľabiny Mt., the bedding of dolomites is oriented SW–NE with about 35–40° dip angle. Measurements show a chaotic joint network oriented mainly in both the NW–SE and W–E directions dipping 70–80°. In the northern part, the dolomite has no bedding and shows a massif blocky structure with NE–SW and SE–NW oriented 50–55° dipping cracks (Fig. 7E).

Geomorphic evidence of DSGSD, which affects mainly the eastern slope of Žľabiny Mt., is present over an area of about 1.2 km^2 and extends 1.7 km in the north-south direction and 1 km in the east-west direction, between 650 and 990 m a.s.l. The deformation is bounded in the east, north, and west by the Zajakovo and Prieseka valleys and in the south by the Malinô Brdo pass. The main ridge of Žľabiny Mt. consists of three subsided blocks at the top (Fig. 7C), bounded by two prominent scarps parallel to the main ridge. The western scarp (Haliny rocks, Fig. 7A) runs from north to south along an elongated karstic aquifer system of cliffs, rock towers, and caves (Fig. 7D, E), intensively affected by gravitational and weathering processes. In some places, typical karstic cavities formed inside the rock. In the rockfall areas and cliffs, gravity-induced caves and extensional corridors are formed as well. The eastern scarp runs along the N–S-oriented main escarpment of DSGSD, with a vertical displacement of few meters below the main ridge (Fig. 7B). It comprises several discontinuous sections from 100 to 500 m long (Fig. 6A). Surface geomorphic features show that the landslide body is divided into three subsided rigid blocks separated by sub-vertical NW–SE fractures or sliding surfaces that appear at different levels on the slope. Furthermore, we found large slope sediment accumulations on slopes with hummocky surfaces and dissected by gullies. The landslide mainly moves NE towards the valley. Two shallow landslides were observed in the lower part of the DSGSD.

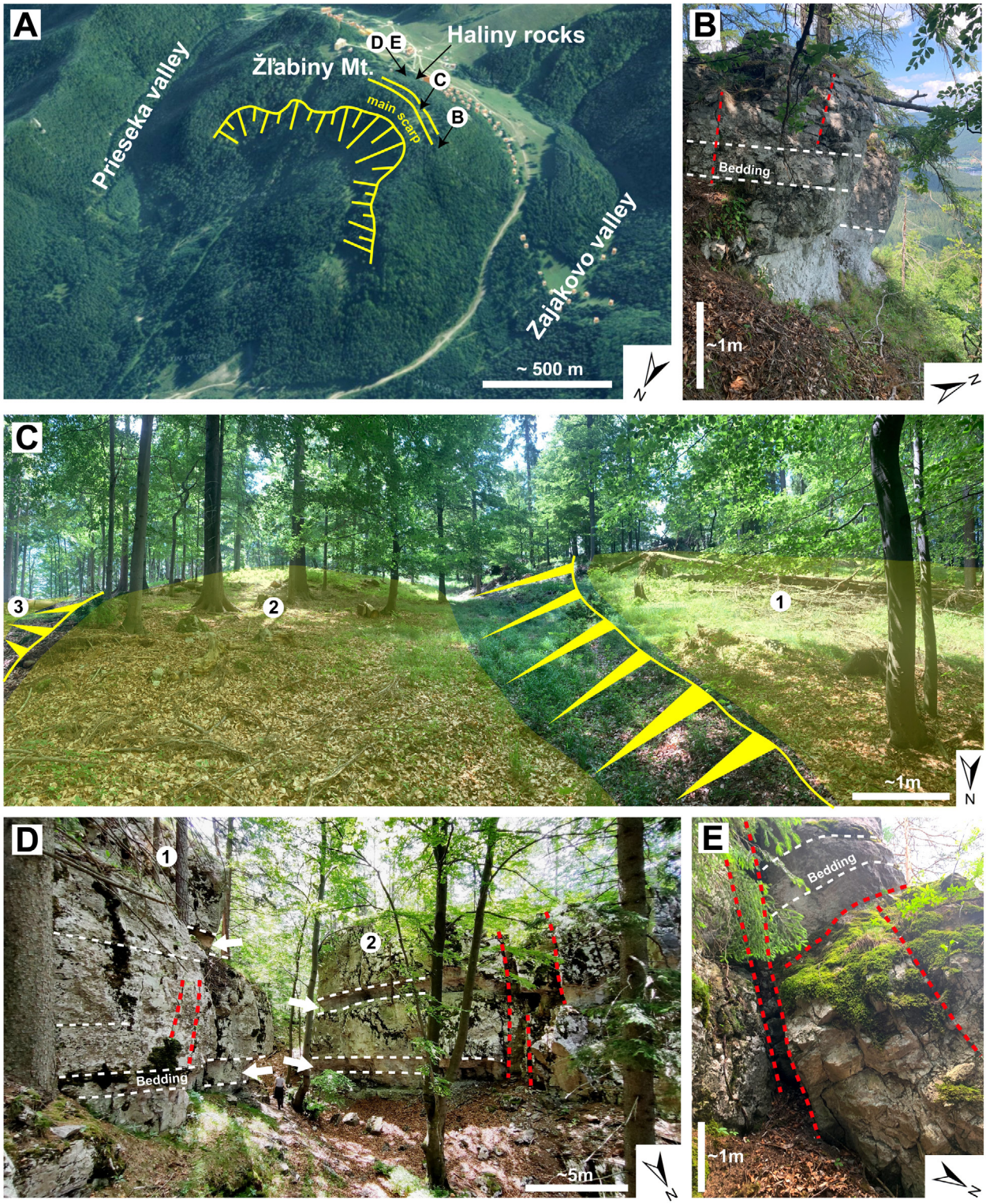

Fig. 7. A — Panoramic 3D view of the Žľabiny mountain and the surrounding areas. Yellow lines show the main scarps. Locations of photos B–E are indicated. **B** — Scarp outcrop in the top of the mountain corresponding to the location d in Fig. 6A. White dashed lines – bedding, red dashed lines – main joints. **C** — Ridge top scarps of DSGSD with visible blocks (1–3). View corresponding to location c in Fig. 6A. **D** — The view of Haliny rocks. White arrows indicate erosional features in the rock mass. 1 – in situ rock block corresponding to the location a in Fig. 6A, 2 – tilted rock block corresponding to the location b in Fig. 6A. **E** — Close-up view of moved and tilted small block in Haliny rocks area.

Numerical modeling results and model evaluation

In this study, the slope geometry, as well as the geomechanical and tectonic properties are considered for the finite element numerical model of the Brdo and Žľabiny DSGSDs. Figure 8 shows the model build-up geometry and boundary conditions, as well as material composition and joints for the Brdo DSGSD (Fig. 8A) and Žľabiny DSGSD (Fig. 8B), which are based on geological cross-sections of both mountains.

Brdo DSGSD

The back-analysis results obtained by the sequential numerical modeling in correspondence with stages 1 and 2 (i.e., the initial and thrust fault stages) show a wide symmetrical shear zone development reaching the yield conditions, with a depth of about 300–400 m and an extent of about 1 km from the mountain top ridge to both sides of the ridge (Fig. 9). In the following stage 3, with added material boundaries corresponding to the collapsed and eroded rock mass, which reaches yield conditions, the entire mountain slope is involved in DSGSD and corresponds well to the portion of the rock mass assumed to have failed to create the present topography. Modeling revealed major principal stresses concentrated within localized landslide toe sectors and a deep underground near the thrust fault area. Less intense stress concentrations also occur at localized spots of the surficial intermediate and lower sectors of the slope on both mountainsides. Moreover, the resulting released zones at the end of the back-thrust stage are associated with vertical failures within the rock mass, with a depth of up to 50 m. The whole released area, as well as the above-mentioned vertical failures, correspond well to the rock mass presently involved in intense rockfall and rockslide processes associated with high-relief slopes. The released rock mass, which is assumed to have been displaced to create the present topography, can be related to landslide phenomena evidenced by visible landslide deposits around the upper part of Brdo Mt. In the final conditions, which correspond to the present topography (stage 4) as a consequence of the widening of the thrust fault-controlled zone, vertical failures caused by a released rock mass that reaches yield conditions occur at distances of up to 1 km from the peak of the mountain.

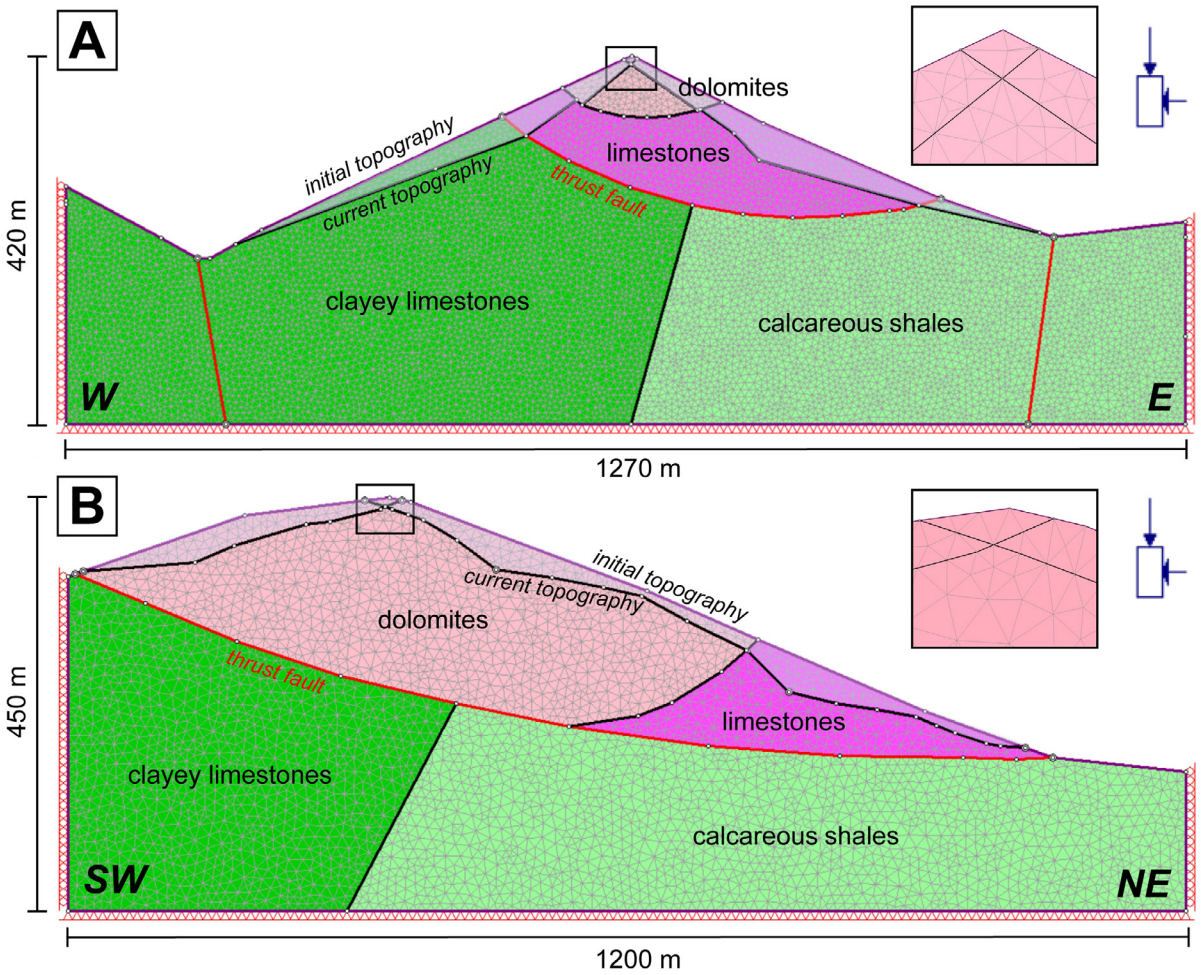

Fig. 8. Model building: **A** — Discretized RS2 model of Brdo slope section with mesh details with assumed initial and current topography. **B** — Discretized RS2 model of Žľabiny slope section with mesh details with assumed initial and current topography.

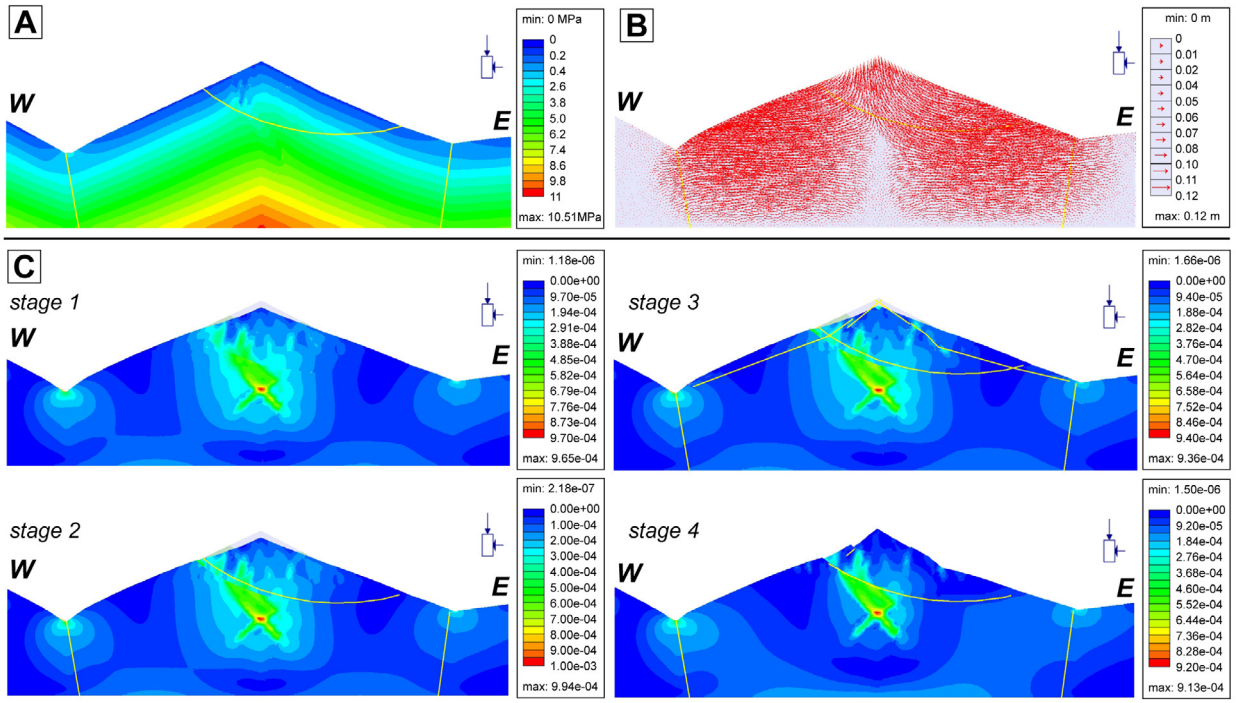

Fig. 9. Finite element simulation results of the Brdo DSGSD: **A** — Sigma 1 stress distribution. **B** — Total displacement vectors. **C** — Maximum shear strain contours: stage 1 – model with assumed initial surface topography before the deformation, stage 2 – initial topography with fault discontinuities, stage 3 – model with added material boundaries between the current topography and eroded/displaced rock mass, stage 4 – model with current topography.

Žľabiny DSGSD

The major principal stress (Sigma 1) distribution shows the behavior of the Žľabiny slope in the vertical direction (Fig. 10A). The total displacement vectors (Fig. 10B) show the increasing displacement on the eastern slope of the mountain, with a maximum value of approximately 25 cm near the landslide toe. The largest vertical displacement was recorded in the peak zone of Žľabiny mountain and the largest horizontal displacement was in the toe zones on both sides of the mountain. The movement is one-sided and oriented downslope. Maximum shear strain analysis revealed the rotational basal shear surface pattern, which follows the thrust fault geometry. In the initial stage 1, without considering any faults, the model predicts the development of two perpendicular shear surfaces similar to the Brdo case (Fig. 10C). However, after introducing the thrust fault discontinuity in stage 2, we observed just one clear shear zone. In stage 3, after introducing surficial material boundaries between the initial and the current surface, it is possible to observe decreasing shear in the central part of the mountain. In stage 4, with the current topography, the clear development of a deep-seated shear zone can be observed in the model.

Parametric analysis

The numerical model and its parametric study allow us to evaluate the influence of rock mass key parameters, as well as mountain geometry on the mechanisms and evolution of DSGSD. To validate and evaluate the accuracy of the models, a comprehensive parametric analysis was conducted. To reduce the number of playing variables and achieve a generalized understanding of DSGSD predispositions, we considered the influence of specific stratigraphic and inherited tectonic features of Brdo Mt. and Žľabiny Mt., which significantly affect the slope deformation and its collapse mechanisms on a local and regional scale. For the same reason, both the initial and current topographies were simplified. When compared to findings from a single-case study, this allowed us to draw more general and robust conclusions about the factors influencing DSGSD evolution. The modeled results of DSGSD's formation and further collapse with deep-seated and shallow landslides correspond well with real-world case studies that had been developed in similar settings. The modeling results suggest that the collapse process could have been predisposed by the thrust fault and later initiated by progressive rock mass strength weakening. The numerical model results showed that the kinematic failure modes derived from the analysis of structural data and current geometry are reasonable. However, it is necessary to highlight that these models remain simplified and conceptual, limited by knowledge of the input parameters and subsurface structure. Conducting sensitivity analyses helped to explore the influence of the critical input parameters on the kinematic behavior of DSGSD. Parameters, such as rock mass deformation modulus (Young's modulus), discontinuity cohesion, and friction angle

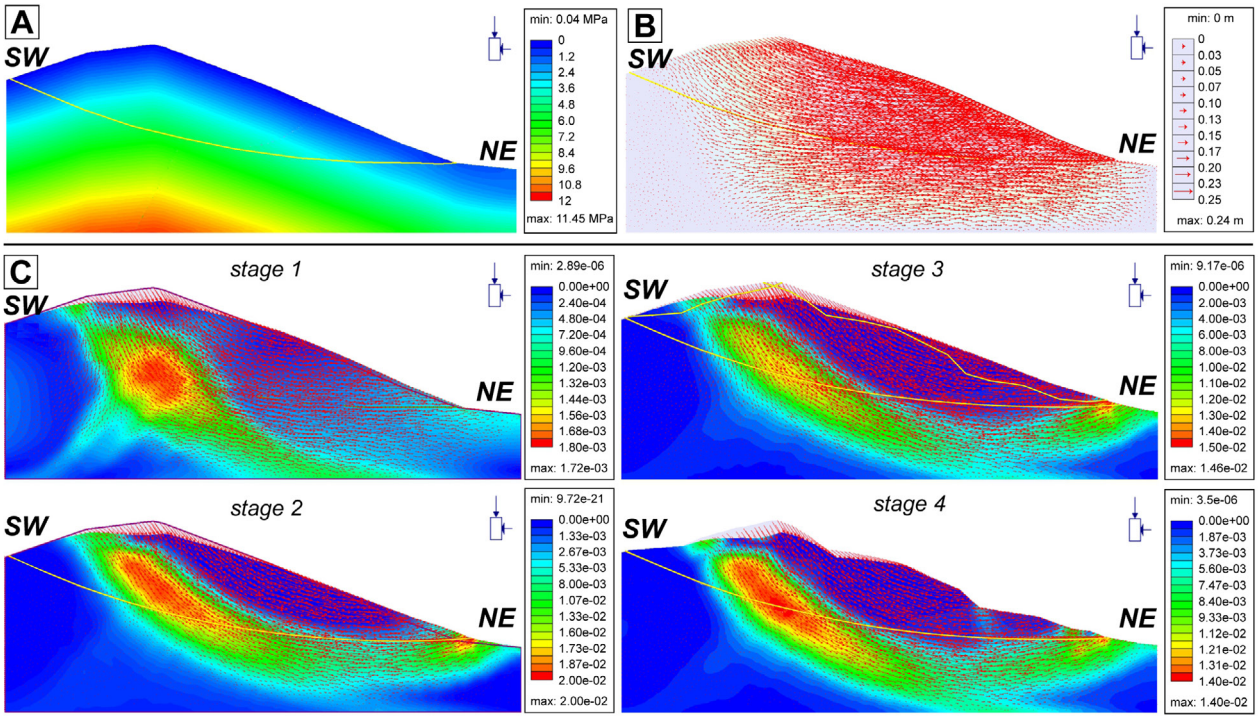

Fig. 10. Finite element simulation results of the Žľabiny DSGSD: **A** — Sigma 1 stress distribution. **B** — Total displacement vectors. **C** — Maximum shear strain contours: stage 1 – model with assumed initial surface topography before the deformation, stage 2 – initial topography with fault discontinuities, stage 3 – model with added material boundaries between the current topography and eroded/displaced rock mass, stage 4 – model with current topography.

were varied between ±25 % of the mean values used for the models in Fig. 8. The outcomes of the parametric analysis are described as a function of total displacement changes in meters (Fig. 11). Young's modulus values of the materials were increased and decreased by 5, 10, and 15 %. The horizontal, vertical, and total displacement, as well as Sigma 1 stress distribution values, were collected using query data points. Using the same principle, we investigated the effect of joint cohesion and joint friction angle on displacement rate (Fig. 11B). In the Brdo case, data points were selected in the deep-seated block, which is separated by a thrust fault (upper block in Fig. 11A) and surficial material mass that was eroded during the development of DSGSD (western block in Fig. 11A). In the Žľabiny case, one deep-seated block separated by a thrust fault from the mountain massif was selected for investigation (Fig. 11A).

Rock mass deformation modulus is a key factor in the overall model displacement. The higher its values, the lower the displacement, and thus the model is more stable. In the Brdo upper block, the mean total displacement changes between 0.08 and 0.06 m, while in the western block, it is between 0.11 and 0.08 m. In the Žľabiny case, the same trend was observed with a mean displacement changing from 0.15 to 0.12 m, when increasing the E values. Still, the analysis results show that the joint cohesion parameter is not an important player in the model's stability. In the Žľabiny case, there are no major changes in the deformation and displacement rates. However, in the Brdo case, the increase of joint cohesion from 0 to 10 MPa caused a slight (0.01 m) decrease in mean displacement. The last tested parameter, the friction angle of the thrust fault discontinuities, shows significant changes in displacement values. The model with a 10-degree friction angle is not stable and collapses in both Brdo and Žľabiny cases. Higher values of the friction angle show a decreasing trend in the displacement from about 0.12 to 0.06 m in the Brdo case. In the Žľabiny case, the decrease in mean displacement is smaller, from 0.14 to 0.12 m.

The conducted parametric analysis on key rock mass design parameters (deformation modulus, cohesion, and friction angle values) shows the main influence of the friction angle on the joints and slip surface development (Fig. 11B). The deformation modulus also has a strong impact on the total displacement of the landslide blocks.

Discussion

Modeling interpretation: evolution and kinematics of studied DSGSDs

It is important to highlight that numerical back-analysis of collapsed DSGSDs can help us to better understand the geomechanical behavior and evolution of slope deformations, even predict their occurrence in similar geological–

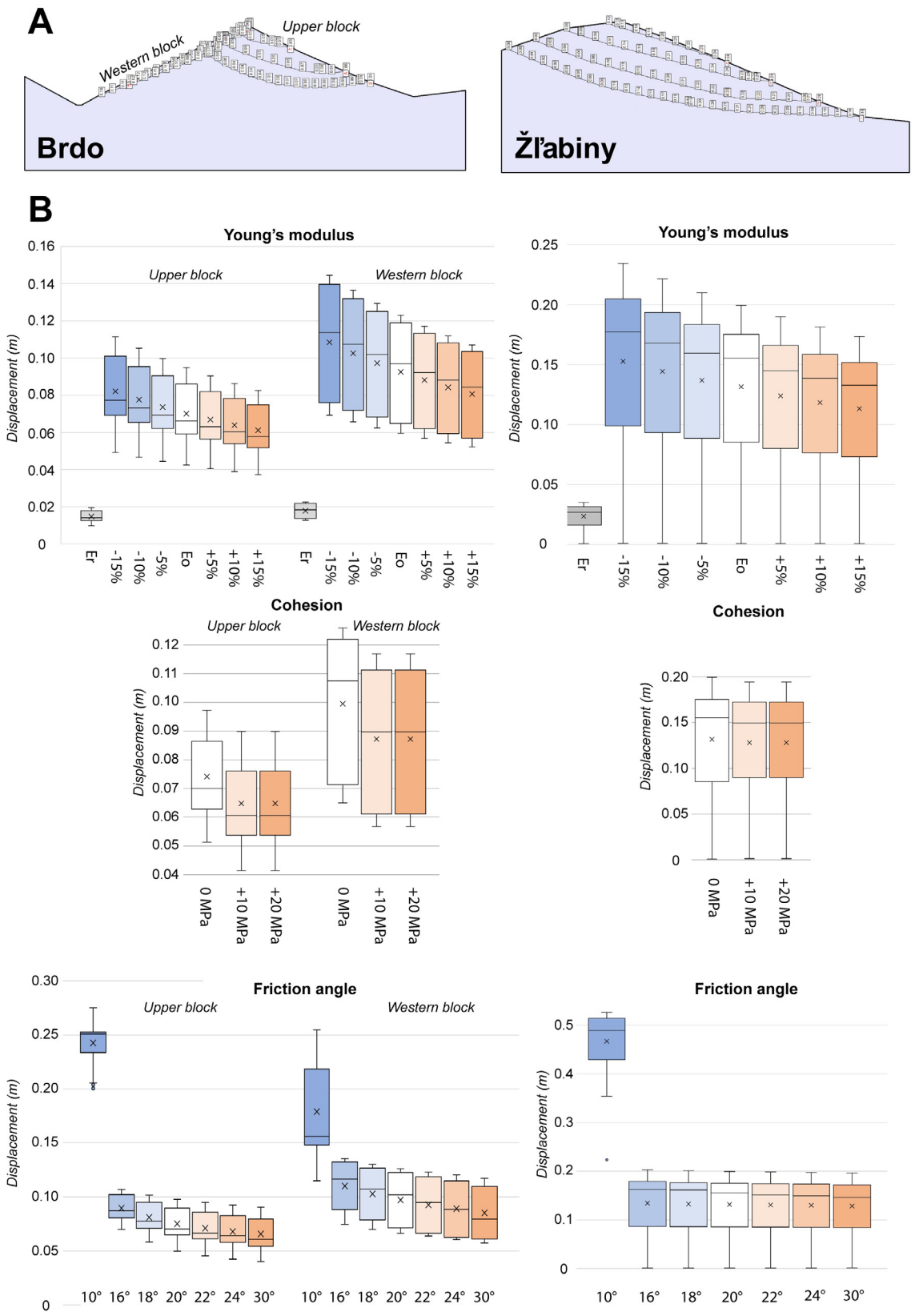

Fig. 11. Parametric analysis of simulated landslides: **A** — Location of query data points in the Brdo and Žľabiny models. **B** — Total displacement boxplots showing the differences which occur by deformation modulus, cohesion and friction angle changes as input parameters. In the chart of Young's modulus *Er* corresponds to a value of intact rock and *Eo* – original value from Table 1, other boxplots there correspond to the *Eo* values increased/decreased by 5, 10 and 15 %.

geomorphic conditions (Bozzano et al. 2012). In this research, we conducted a 2D finite element analysis on two topographically different collapsed DSGSDs to describe their possible stress-strain regime and their changes during the different development stages of deformation. Through the numerical modeling of the Brdo and Žľabiny DSGSDs, we were able to reconstruct the main evolutionary phases and infer the primary predisposing factors, as well as the kinematics of the deformation. The modeling outcomes correspond with the geomorphological field data, as well as with remote sensing data interpretation. They highlight the kinematic components of DSGSDs and the strong control of inherited structural features as a crucial basis for the model's development. The evolution of the Brdo DSGSD could be explained as a continuous sequence of slope movements (Fig. 12). With regards to the field evidence of existing troughs, scarps, and antislope scarps parallel to the ridge, it is possible to assume that the Brdo DSGSD is a symmetric case of sackung with two deep-reaching slip surfaces and one down-dropped keystone block on the top of the mountain (Fig. 12C). The evolution model of the Žľabiny DSGSD based on the numerical model shows the activation of two initial deep-seated shear planes, as well as further deactivation of one of them (Fig. 13). The upper part of the landslide developed into the rockfall areas, which evolved later into the current Haliny rocks (Fig. 13B, C). The geometry and synclinal structure of the mountain predisposed the main deep-seated landslide development and a slope deformation scenario thus followed. According to this interpretation, one deep block moved downslope on the eastern flank of the mountain and later, a second rock mass block followed it because of the secondary shear zone development near the surface (Fig. 13C). The studied DSGSDs demonstrate geotechnically and temporally complicated failures and deformation processes, distinguished by the sequential movement of individual rock slide slabs. A parametric study of all 4 model stages revealed the ranges of the main rock mass characteristics values (cohesion, friction angle, and deformation modulus)

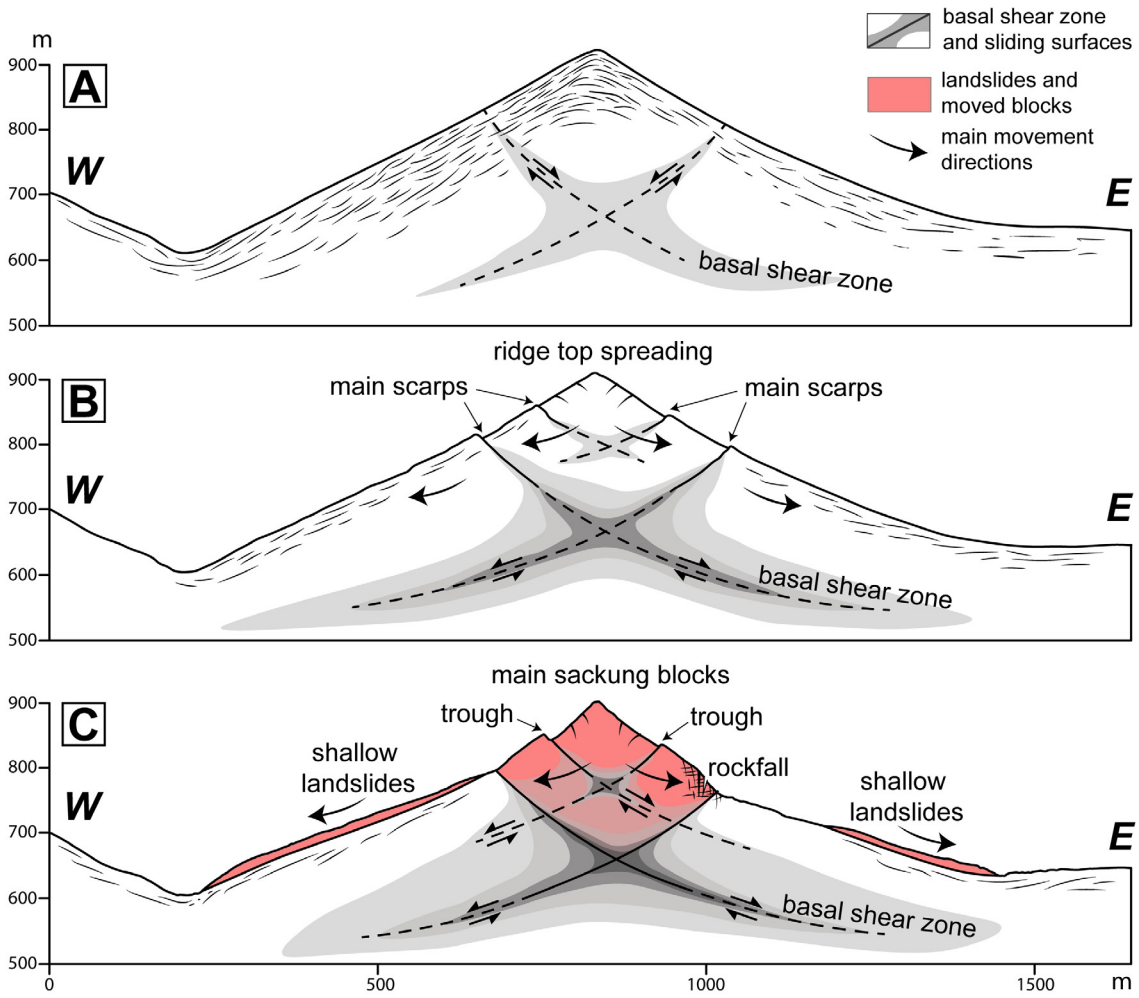

Fig. 12. Conceptual model of Brdo DSGSD evolution: **A** — Initial stable slope conditions with pre-failure topography of Brdo mountain along the cross-sectional profile and the development of deep shear zones. **B** — Basal shear zone formation and development of main scarp areas. **C** — Main symmetric sackung formation. Internal main discontinuities are developed, separating the rock mass into a few blocks.

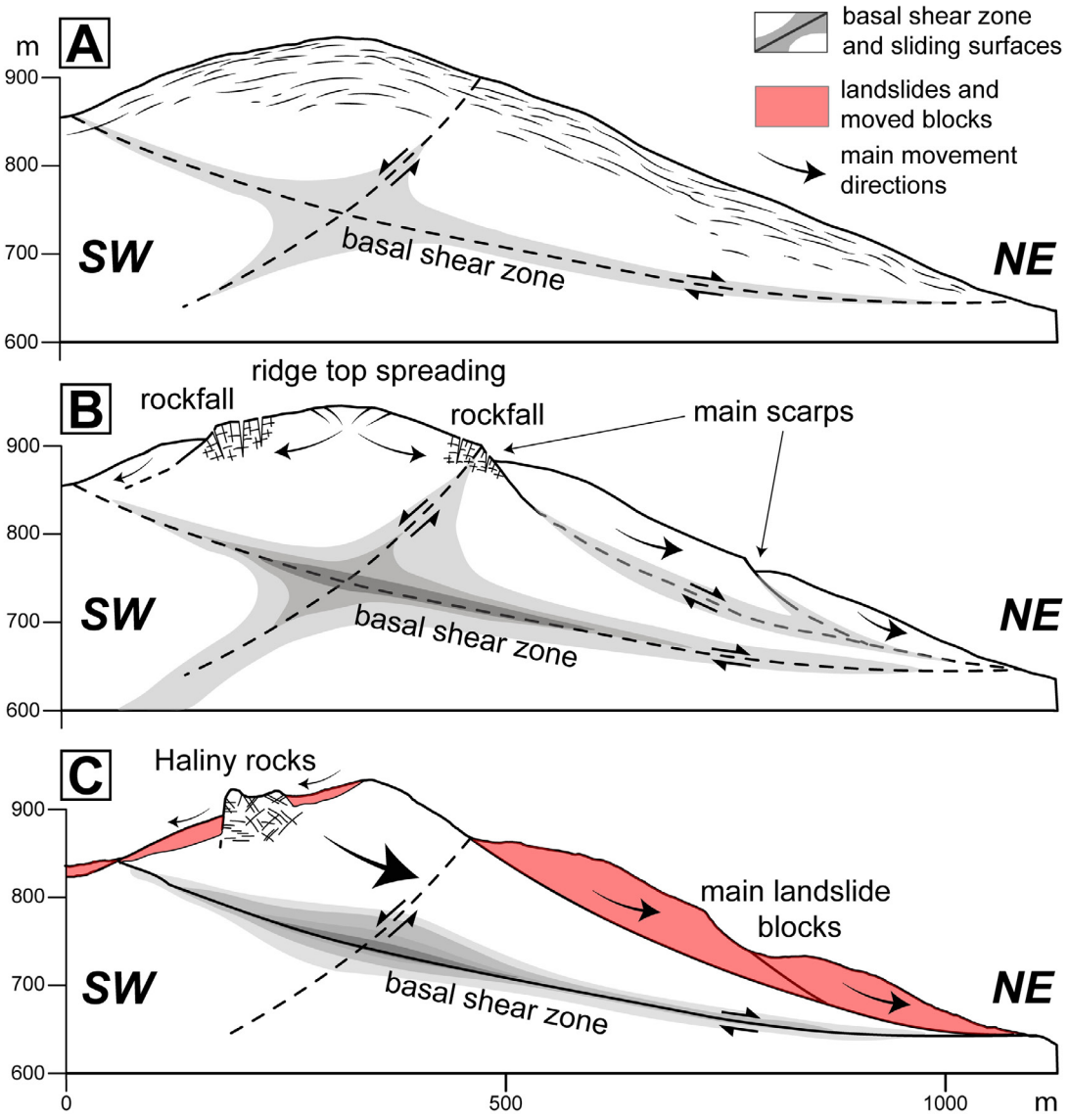

Fig. 13. Conceptual model of the Žľabiny DSGSD evolution: **A** — Initial stable slope conditions with pre-failure topography and the development of deep shear zones. **B** — Basal shear zone formation and development of rockfall areas. **C** — Collapse of DSGSD. Internal main discontinuities are developed, separating the rock mass into a few blocks.

which produce validated harmonic model behavior during the stress-strain analysis.

Causes of studied DSGSDs

A detailed understanding of the predisposition, preparatory, and triggering factors of DSGSDs and their collapses is a critical aspect of the analysis of such complex phenomena. In the Carpathians, including the Veľká Fatra Mts., we face growing anthropogenic pressures that can cause an increase in DSGSD collapse hazards (Skrzypczak et al. 2021). Previous DSGSD research in Slovakia and other regions has identified causal factors at the local and regional levels and were focused on the active ongoing DSGSD cases (Briestenský et al. 2011; Baroň et al. 2019; Crippa et al. 2020). The fact that the area has never been glaciated allows us to exclude glacial and post-glacial dynamics in predisposition. We thus consider other factors, including inherited and other morphodynamic controls, as possible DSGSD predispositions. Inherited tectonic and morphostructural predispositions are one of the major causal factors in both the Brdo and Žľabiny DSGSDs. The faulted and folded limestone/dolomite layers combined with a major thrust create favorable conditions for deep movement and instability scenarios along main discontinuity planes. The tectonic predisposing factor corresponds with field observations in DSDSDs, as well as to similar case studies around the other European orogenic belts (Baroň et al. 2019; Faccini et al. 2020; Aringoli et al. 2021; Discenza et al. 2023). Deformability contrasts between the underlying (softer) and overlying (rigid) rock formations that had been reinforced

by karstification processes and specific hydrogeological conditions, as well as fluvial incision along the slope toes, could also be considered possible predisposing factors (Briestenský et al. 2011; Discenza & Esposito 2021). After initial deep gravitational movements along the inherited thrust fault, the shear zone developed and involved larger areas of the mountain rock massif. This could be considered gravitational rejuvenation of the thrust fault, which represents a process comparable to the results of other studies performed previously in the Carpathians (Pánek et al. 2011, 2013; Sikora 2022). According to our results, gravitational processes were included in the further development of more shallow shear zones which separated mountain massif into blocks and started the main DSGSD collapse. The topography (slope geometry) influenced slightly different scenarios for the development and collapse of the DSGSDs. In the Brdo case, the separated, blocky structures moved symmetrically downwards from the mountain crest and created upper and lower DSGSD areas with cliffs and deep troughs between them. The upper part was also disintegrated and typical sackung features with mountain-ridge spreading and antislope scarps appeared in the area (Fig. 12). In the Žľabiny area, the deep shear surface developed into an eastward-deepening slip zone with several more surficial shear zones on the eastern side of the mountain. Topographical stresses and slope critical state likely provoked the deep-seated landslide occurrence which caused a collapse of the Žľabiny DSGSD. A few deep-seated rock mass blocks moved towards the valley side (Fig.13).

As we did not conduct any chronological analyses, we can only assume the probable triggering factors of the episodic deformations that contributed to the deep gravitational creep. Slovakia is a region with moderate-to-low seismic activity, but several historical earthquakes with local magnitude >4 have been recorded in the country since the onset of instrumental measurements (Csicsay et al. 2018). Moreover, extreme rainfall events are considered to be a major factor provoking slope movements in the Carpathians (Pánek et al. 2013, 2016). The shallow landslide/rockfall deposits all around the studied mountains show intense weathering of rock from the upper slope sections and its transportation to the valleys. Shallow landslides and rockfalls could thus be predisposed by rock weathering and bedrock fragmentation and triggered by extreme hydroclimatic events or earthquakes.

We can argue that for settings similar to our case study, a combined action of pre-existing thrust fault, morphostructural, and topographic conditions could be considered a predisposing factor. The seismic, climatic, and hydrogeologic players also could be included just as a triggering factor. The progressive weakening of the rock mass and the reach of a critical state of the slope can eventually result in a major reactivation triggered by a seismic or hydroclimatic event. Alternatively, fluvial incision, particularly along slopes with substantial local relief, may disrupt the equilibrium of stability, further intensifying the likelihood of failure.

The model and analysis results agree with field observations and other DSGSD case studies from the nearby High Tatra Mts. (Králiková et al. 2014a; Pánek et al. 2016), and suggest a strong influence of gravitational-tectonic control on deep-slope movements in the region. The results of this study add a piece to the mosaic of the Quaternary gravitational morphogenesis of Central Western Carpathians, highlighting the role of passive morpho-structural control on high-relief gravitational deformations in the Veľká Fatra Mts. There are wide possibilities to deepen the understanding of collapsed DSGSD by more detailed borehole, geophysical, and remote sensing investigations of this area, as well as exploring the widely-mapped DSGSD cases around the Carpathian Mountains.

Conclusions

In this paper, the characteristics, predisposing factors, and failure mechanisms of the Brdo and Žľabiny DSGSDs in the Veľká Fatra Mts., Slovakia, were investigated by remote sensing data interpretation, fieldwork, and numerical modeling. The finite element numerical modeling approach presented here allows us to analyze the main evolutionary stages of relatively small mountain areas affected by DSGSD through a stress-strain sequential numerical model based on detailed geomorphological, geological-structural, and geomechanical data. Several conclusions can be drawn from this study:

The landslides occur in the active Alpine tectonic region of the Veľká Fatra Mts. Due to the previous tectonic evolution, the geological structure is characterized by thrust-faulted, folded, and weathered dolomite and limestone rocks that are favorable for karst processes. The geological, topographic, and climatic conditions were beneficial for DSGSD and landslide development.

The numerical model analysis indicated that among the predisposing causes of DSGSDs, the thrust fault structure was a predominant contributing factor. The initial topography also influenced the geometry of DSGSDs: in the symmetric Brdo case, the mass movement evolved into the symmetric sackung, while in the elongated Žľabiny case, DSGSD developed to block movements on the eastern side of the mountain. In general, the modeling does not support the hypothesis of a DSGSD collapse of the Brdo and Žľabiny mountains under gravity alone.

These findings could provide a good starting point for further numerical modeling applications in the natural high-relief stability problems and give insight into a deeper and more detailed investigation of DSGSDs around the Central Western Carpathians.

Acknowledgments: The study was conducted within the framework of the University of Ostrava projects SGS02/PřF/2023, SGS02/PřF/2024, and SGS02/PřF/2025. We gratefully acknowledge Francisco Gutiérrez and two anonymous reviewers for their valuable comments which substantially improved the manuscript.

References

Agliardi F., Crosta G.B. & Frattini P. 2013: Slow rock-slope deformation. In: Clague J.J. & Stead D. (Eds.): Landslides: Types, Mechanisms and Modeling. *Cambridge University Press*, Cambridge, 207–221. https://doi.org/10.1017/CBO9780511740367.019

Aringoli D., Farabollini P., Pambianchi G., Materazzi M., Bufalini M., Fuffa E., Gentilucci M. & Scalella G. 2021: Geomorphological Hazard in Active Tectonics Area: Study Cases from Sibillini Mountains Thrust System (Central Apennines). *Land* 10, 510. https://doi.org/10.3390/land10050510

Baroň I., Sokol L., Melichar R. & Plan L. 2019: Gravitational and tectonic stress states within a deep-seated gravitational slope deformation near the seismogenic Periadriatic Line fault. *Engineering Geology* 261, 105284. https://doi.org/10.1016/j.enggeo.2019.105284

Bednarik M., Magulová B., Matys M. & Marschalko M. 2010: Landslide susceptibility assessment of the Kraľovany – Liptovský Mikuláš railway case study. *Physics and Chemistry of the Earth* 35, 162–171. https://doi.org/10.1016/j.pce.2009.12.002

Bertuzzi R., Douglas K. & Mostyn G. 2016: Comparison of quantified and chart GSI for four rock masses. *Engineering Geology* 202, 24–35. https://doi.org/10.1016/j.enggeo.2016.01.002

Bozzano F., Martino S., Montagna A. & Prestininzi A. 2012: Back analysis of a rock landslide to infer rheological parameters. *Engineering Geology* 131–132, 45–56. https://doi.org/10.1016/j.enggeo.2012.02.003

Briestenský M., Košťák, B., Stemberk J. & Vozár J. 2011: Long-term slope deformation monitoring in the high mountains of the Western Carpathians. *Acta Geodynamica et Geomaterialia* 4, 403–412.

Crippa C., Franzosi F., Zonca M., Manconi A., Crosta G.B., Dei Cas L. & Agliardi F. 2020: Unraveling spatial and temporal heterogeneities of very slow rock-slope deformations with targeted DInSAR analyses. *Remote Sensing* 12, 1329. https://doi.org/10.3390/rs12081329

Crosta G. 1996: Landslide, spreading, deep seated gravitational deformation: analysis, examples, problems and proposal. *Geografia Fisica e Dinamica Quaternaria* 19, 297–313.

Csicsay K., Cipciar A., Fojtíková L., Kristeková M., Gális M., Srbecký M., Chovanová Z., Bystrický E. & Kysel R. 2018: The National Network of Seismic Stations of Slovakia – Current state after 13 years in operation from the project of modernization and enhancement. *Contributions to Geophysics and Geodesy* 48, 337–348. https://doi.org/10.2478/congeo-2018-0016

Discenza M.E. & Esposito C. 2021: State-of-art and remarks on some open questions about DSGSDs: hints from a review of the scientific literature on related topics. *Italian Journal of Engineering Geology and Environment* 1, 31–59. https://doi.org/10.4408/IJEGE.2021-01.O-03

Discenza M.E., Esposito C., Komatsu G. & Miccadei E. 2021: Large-scale and deep-seated gravitational slope deformations on Mars: a review. *Geosciences* 11, 174. https://doi.org/10.3390/geosciences11040174

Discenza M.E., Di Luzio E., Martino S., Minnillo M. & Esposito C. 2023: Role of inherited tectonic structures on gravity-induced slope deformations: inference from numerical modeling on the Luco dei Marsi DSGSD (Central Apennines). *Applied Sciences* 13, 4417. https://doi.org/10.3390/app13074417

Dramis F. & Sorriso-Valvo M. 1994: Deep-seated gravitational slope deformations, related landslides and tectonics. *Engineering Geology* 38, 231–243.

Esri 2023: ArcGIS Pro, version 3.4, software.

Faccini F., Federico L., Torchio S., Roccati A., Capponi G. & Crispini L. 2020: A mountain slope deformation in an alpine metaophiolitic massif (Ligurian Alps, Italy). *Journal of Maps* 17, 77–89. https://doi.org/10.1080/17445647.2020.1854130

Földvary G.Z. 2009: The Carpathian Mountain range and the enclosed interior. *Central European Journal of Geosciences* 1, 291–302. https://doi.org/10.2478/v10085-009-0024-5

GKÚ Bratislava, NLC 2024: Orthophotomosaic of Slovakia. *National Forest Centre and Geodetic and Cartographic Institute Bratislava*. https://www.geoportal.sk/en/zbgis/orthophotomosaic/ (accessed 2024-12-27).

Hoek E. & Diederichs M.S. 2006: Empirical estimation of rock mass modulus. *International Journal of Rock Mechanics & Mining Sciences* 43, 203–215.

Hoek E., Carranza-Torres C. & Corkum B. 2002: Hoek-Brown failure criterion. *Proc. NARMS-TAC Conference, Toronto* 1, 267–273.

Hoek E., Carter T.G. & Diederichs M.S. 2013: Quantification of the Geological Strength Index chart. *47th US Rock Mechanics/Geomechanics Symposium* (ARMA 13-672, San Francisco, CA, USA).

Kočický D. & Ivanič B. 2011: Geomorphological division of Slovakia 1:50,000. *State Geological Institute of Dionýz Štúr*, Bratislava (in Slovak).

Kohút M. & Larionov A.N. 2021: From subduction to collision: Genesis of the Variscan granitic rocks from the Tatric Superunit (Western Carpathians, Slovakia). *Geologica Carpathica* 72, 96–113. https://doi.org/10.31577/GeolCarp.72.2.2

Kohút M., Carl C. & Michalko J. 1996: Granitoid Rocks of the Veľká Fatra Mts. Rb/Sr Isotope Geochronology (Western Carpathians, Slovakia). *Geologica Carpathica* 47, 81–89.

Kopecký M., Ondrášik M. & Antolová D. 2012: Atlas of landslides in Slovakia. *AGH Journal of Mining and Geoengineering* 36, 211–217.

Kováč M., Kráľ J., Márton E., Plašienka D. & Uher P. 1994: Alpine uplift history of the Central Western Carpathians: Geochronological, paleomagnetic, sedimentary and structural data. *Geologica Carpathica* 45, 83–96.

Králiková S., Vojtko R., Sliva Ľ., Minár J., Fügenschuh B., Kováč M. & Hók J. 2014a: Cretaceous-Quaternary tectonic evolution of the Tatra Mts. (Western Carpathians): constraints from structural, sedimentary, geomorphological, and fission track data. *Geologica Carpathica* 65, 307–326. https://doi.org/10.2478/geoca-2014-0021

Králiková S., Vojtko R., Andriessen P., Kováč M., Fügenschuh B., Hók J. & Minár J. 2014b: Late Cretaceous–Cenozoic thermal evolution of the northern part of the Central Western Carpathians (Slovakia): Revealed by zircon and apatite fission track thermochronology. *Tectonophysics* 615–616, 142–153. https://doi.org/10.1016/j.tecto.2014.01.002

Kromuszczyńska O., Mège D., Dębniak K., Gurgurewicz J., Makowska M. & Lucas A. 2019: Deep-seated gravitational slope deformation scaling on Mars and Earth: Same fate for different initial conditions and structural evolutions. *Earth Surface Dynamics* 7, 361–376. https://doi.org/10.5194/esurf-7-361-2019

Lebourg T., Zerathe S., Fabre R., Giuliano J. & Vidal M. 2014: A Late Holocene deep-seated landslide in the northern French Pyrenees. *Geomorphology* 208, 1–10. https://doi.org/10.1016/j.geomorph.2013.11.008

Lepeška T. 2016: Dynamics of development and variability of surface degradation in the subalpine and alpine zones (an example from the Velká Fatra Mts., Slovakia). *Open Geosciences* 8, 771–786. https://doi.org/10.1515/geo-2016-0056

Maglay J., Halouzka R., Baňacký V., Pristaš J., Janočko J. & Hók J. 1999: Neotectonic map of Slovakia 1:500,000. *Slovak Geological Survey*, Bratislava.

Malgot J. 1977: Deep-seated gravitational slope deformations in neovolcanic mountain ranges of Slovakia. *Bulletin of Engineering Geology and the Environment* 16, 106–109.

Malík P., Coplák M., Kuvik M. & Švasta J. 2019: Recharge Impulse Spreading in Western Carpathian's Mountainous Fissure–Karst Aquifer. *Water* 11, 763. https://doi.org/10.3390/w11040763

Matula M. & Nemčok A. 1966: Overview of landslide processes in Slovakia. *Inžinierske Stavby* 14, 29–30 (in Slovak).

Pánek T., Táborík P., Klimeš J., Komárková V., Hradecký J. & Šťastný M. 2011: Deep-seated gravitational slope deformations in the highest parts of the Czech Flysch Carpathians: evolutionary model based on kinematic analysis, electrical imaging and trenching. *Geomorphology* 129, 92–112. https://doi.org/10.1016/j.geomorph.2011.01.016

Pánek T., Smolková V., Hradecký J., Baroň I. & Šilhán K. 2013: Holocene reactivations of catastrophic complex flow-like landslides in the Flysch Carpathians (Czech Republic/Slovakia). *Quaternary Research* 80, 33–46. https://doi.org/10.1016/j.yqres.2013.03.009

Pánek T., Engel Z., Mentlík P., Braucher R., Březný M., Škarpich V. & Zondervan A. 2016: Cosmogenic age constraints on post-LGM catastrophic rock slope failures in the Tatra Mountains (Western Carpathians). *Catena* 138, 52–67. https://doi.org/10.1016/j.catena.2015.11.005

Plašienka D. 2018: Continuity and episodicity in the early Alpine tectonic evolution of the Western Carpathians: How large-scale processes are expressed by the orogenic architecture and rock record data. *Tectonics* 37, 2029–2079. https://doi.org/10.1029/2017TC004779

Polák M., Bujnovský A. & Kohút M. 1997: Geological map of Veľká Fatra Mts. 1:50,000. *Slovak Geological Survey*, Bratislava (in Slovak).

Radbruch-Hall D.H. 1978: Gravitational creep of rock masses on slopes. In: Voight B. (Ed.): Rockslides and avalanches. Natural phenomena – developments in geotechnical engineering. *Elsevier* 14, 607–657.

Rocscience Inc. 2019: RS2, version 9.030, software.

Sikora R. 2022: Geological and geomorphological conditions of landslide development in the Wisła source area of the Silesian Beskid mountains (Outer Carpathians, southern Poland). *Geological Quarterly* 66, 19.

Šimeková J. & Martinčeková T. (Eds.) 2006: Atlas of slope stability maps SR 1:50,000. *State Geological Institute of Dionýz Štúr*, Bratislava, 1–155 (in Slovak).

Šimeková J., Liščák P., Jánová V. & Martinčeková T. 2014: Atlas of Slope Stability Maps of the Slovak Republic at Scale 1:50,000 – Its Results and Use in Practice. *Slovak Geological Magazine* 14, 19–30.

Skrzypczak I., Kokoszka W., Zientek D., Tang Y. & Kogut J. 2021: Landslide Hazard Assessment Map as an Element Supporting Spatial Planning: The Flysch Carpathians Region Study. *Remote Sensing* 13, 317. https://doi.org/10.3390/rs13020317

Sorriso-Valvo M., Gullà G., Antronico L., Tansi C. & Amelio M. 1999: Mass-movement, geologic structure and morphologic evolution of the Pizzotto-Greci slope Calabria, Italy. *Geomorphology* 30, 147–163.

ÚGKK SR 2024: Airborne Laser Scanning – DTM. *Geodesy, Cartography and Cadastre Authority of the Slovak Republic*. https://www.geoportal.sk/en/zbgis/als/ (accessed 2024-12-27).

Wallace C.S., Schaefer L.N. & Villeneuve M.C. 2022: Material Properties and Triggering Mechanisms of an Andesitic Lava Dome Collapse at Shiveluch Volcano, Kamchatka, Russia, Revealed Using the Finite Element Method. *Rock Mechanics and Rock Engineering* 55, 2711–2728. https://doi.org/10.1007/s00603-021-02513-z

Wang H., Lin H. & Cao P. 2017: Correlation of UCS Rating with Schmidt Hammer Surface Hardness for Rock Mass Classification. *Rock Mechanics and Rock Engineering* 50, 195–203. https://doi.org/10.1007/s00603-016-1044-7